World Journal of Environmental Biosciences
Available Online at: **www.environmentaljournals.org**

Volume 15, Issue 1: 228-240

https://doi.org/10.51847/t5onQUNz30

ISSN 2277- 8047

Assessing Green Biomass and Undergrowth in Amankaragay Pine Forest Using Unmanned Aerial Vehicles and Machine Learning

Seitbek Kuanyshbayev[1], Aliya Yskak[1], Bekmyrza Zhumash[1]*, Almabek Nugmanov[1], Gulnaz Yermoldina[1], Vladimir Fominov[1], Andrey Kupriyanov[2], Oleg Kuprijanov[2], Petr Lyanga[1], Adil Nurpeisov[1], Yevgeniy Sokharev[3], Zhanna Suimenbayev[4], Akhmet Bugubaev[1], Zayna Zhussupbekova[5]

[1]Akhmet Baitursynuly Kostanay Regional University, Kostanay, Republic of Kazakhstan.
[2]Kuzbass Botanical Garden Russian Federal State Research Center of Coal and Coal Chemistry, Siberian Branch of the Russian Academy of Sciences, Novosibirsk, Russian Federation.
[3]Municipal State Company "Kostanay Regional Pathoanatomical Bureau" of the Health Department of the Akimat of the Kostanay Region, Kostanay, Kazakhstan.
[4]Institute of Information and Computing Technologies, Almaty, Kazakhstan.
[5]National Institute of Intellectual Property, Astana, Kazakhstan.

ABSTRACT

This study examined the potential of unmanned aerial vehicles to assess green biomass and undergrowth density in areas of the Amankaragay pine forest affected by the catastrophic fires of 2022. Comparative characteristics were obtained for two variants of the Random Forest model on homogeneous and heterogeneous sites. The proposed approach enabled the generation of high-precision distribution maps of birch undergrowth and other vegetation types. The study recommended that, to improve the accuracy of the Modified Mode and Basic Model methods, additional investigation of undergrowth areas in multispectral ranges should be carried out to examine the influence of plant physiological indices. In the analyzed areas, covering approximately 10 hectares, we determined the density of birch undergrowth. The average value was 0.0022 per 1 m^2. On heterogeneous sites, the Modified Mode model error was about 85%, while the Basic Model error was about 95%. The developed technology can substantially increase the speed, detail, and reliability of forest stand assessment without labor-intensive ground surveys. The obtained results are of significant practical importance for forest restoration, monitoring, and forest ecosystem management, demonstrating the potential of modern UAVs and machine learning methods for rapid vegetation assessment at the landscape level.

Keywords: *Multispectral photo and video surveying, Remote sensing, Forest inventory, Vegetation, Plant physiological index, Automated monitoring*

Corresponding author: Bekmyrza Zhumash
e-mail ✉ zh.bekmyrza@mymail.academy
Received: 26 August 2026
Accepted: 30 September 2026

INTRODUCTION

Over the past two decades, Jolly *et al.* (2015) and Van der Werf *et al.* (2017) report that fire-danger seasons have become more frequent, leading to a significant rise in fires globally. Thus, from 2023 to 2024, approximately 3.9 million km^2 were burned. As a result, assessing the state of post-fire ecosystems requires more resources, creating economic costs and demanding highly qualified specialists and equipment. The scale of the fires in Kostanay Region in the first half of September 2022 had no precedent. Abnormally high September temperatures exceeding 36 °C, together with the absence of rainfall, created difficult fire conditions in Kostanay Region. The fires damaged 43 thousand hectares of forest land in Kostanay Region (Akhmet, 2022; Bolbot, 2022; Dosanova, 2022; Makarov, 2022; Nasha Gazeta., 2022; Official website of the President of the Republic of Kazakhstan., 2022; Sputnik., 2022). High temperature and reduced humidity are among the key factors in fire formation. Restoring forests affected by fires is an extremely complex, long-term process. Successional processes may also involve changes in the original species composition, which is particularly dangerous for relict forests. Discussion of forest restoration in Northern Kazakhstan after fires is therefore highly relevant (Kupriyanov *et al.*, 2003; Dancheva *et al.*, 2015; Makhanova *et al.*, 2022). Several studies describe the pine relict forest of Kostanay Region (Gribanov, 1960; Pugachev, 1994).
During 2024–2025, the authors of the present study conducted multifactorial ecological research to assess the restoration of the pine relict forest of Kostanay Region affected by fires. The authors have practical experience in assessing the restoration of forest ecosystems after fires (Kupriyanov *et al.*, 2003), assessing the recovery of vegetation cover on lands affected by

World Journal of Environmental is an open access journal, and articles are distributed under the terms of the Creative Commons Attribution-Non Commercial-ShareAlike 4.0 License, which allows others to remix, tweak, and build upon the work non-commercially, as long as appropriate credit is given and the new creations are licensed under the identical terms. (https://creativecommons.org/licenses/by-nc-sa/4.0/).

technogenic impact (Nugmanov *et al.*, 2022; Bugubaeva *et al.*, 2023; Chashkov *et al.*, 2024), and organizing and conducting assessments of environmental monitoring objects using Earth remote sensing methods, including specialized unmanned systems and satellite remote sensing data (Chashkov *et al.*, 2023; Zarubin *et al.*, 2025a; 2025b).

Currently, developing and implementing methods to assess and inventory the condition of forest systems is a regulatory requirement and highly relevant (Wikipedia, the free encyclopedia., n.d.; Parliament of the Republic of Kazakhstan., 2003). Modern assessment methods mostly include ground-based monitoring of undergrowth recovery, which is difficult to perform over large areas. Against the backdrop of fires, there is a growing need for methods that allow rapid, accurate assessment of forest ecosystem conditions using remote sensing methods and tools.

UAV-based imagery offers methods for reconstructing plant species conditions using remote sensing techniques. Obtaining a primary RGB assessment, that is, an image assessment based on three color channels, makes it possible to determine the number and density of undergrowth and its morphological characteristics. This is a relevant problem because large fires are increasingly common (Banskota *et al.*, 2014; Van der Werf *et al.*, 2017; Bousquet *et al.*, 2022). In addition, machine learning methods have previously demonstrated effectiveness in analyzing orthophotoplans, significantly accelerating data analysis and reducing human error.

Global trends increasingly involve remote sensing methods for assessing and monitoring forest ecosystems. Related conceptual work has proposed detecting beaver settlement sites from satellite and UAV imagery to support monitoring of forest ecosystems (Logachev, 2024). Traditional approaches are limited by the time required for manual assessment. Satellite-based approaches are limited by maximum resolution, where a single pixel may represent several trees, which affects the quality of forest system assessment. Kleinsmann *et al.* (2023) discussed satellite image quality issues and the potential of drone technology. The authors considered new possibilities for monitoring forest systems. The study demonstrated high accuracy in tree segmentation using multispectral images, with an F-score of 0.92 for deciduous trees, 1.0 for coniferous trees, and an overall mean F-score of 0.79; however, it identified limitations in heterogeneous areas. In addition to Kleinsmann *et al.* (2023), this study focuses on assessing and inventorying undergrowth density during post-fire ecosystem recovery, where assessment may be complicated by partial overlap, small crowns, and substantial noise from understory vegetation.

UAVs bring researchers closer to analyzing each tree individually, although computational resources, imaging seasons, detail, and site homogeneity limit such methods. UAV use is an effective monitoring method, especially when combined with machine learning technologies, including basic algorithms, deep learning algorithms, and convolutional neural networks. In Gan *et al.* (2023) and Xi *et al.* (2024), various methods and model architectures were compared for heterogeneous forest assessment, and accuracy varied by tree species. In the present article, the models have the following characteristics: DeepForest — F-score = 0.52, Detectree2 — F-score = 0.57, Random Forest — F-score = 0.71, ResNet — F-score = 0.84, and SegFormer — F-score = 0.89. These results reflect the advantage of deep learning for in-depth assessment and may be used to assess strictly protected tree species.

One of the most significant studies for the present research is Feduck *et al.* (2018), which examines in detail the use of UAVs for detecting coniferous undergrowth on an orthophotoplan, or orthomosaic. This work also became an important reference point for selecting methodologies and approaches for data assessment and analysis. In Feduck *et al.* (2018), the study used high-quality RGB images and red-edge imagery, an additional image channel in the operating range of 680–730 nm. The authors note that automation reduces assessment labor costs compared with traditional ground-based methods and achieved an efficiency of 75.8% using the CART algorithm (Feduck *et al.*, 2018).

In the present study, we directly compared the automated method with manual validation for rapid field inventory tasks. This required a method suitable for applied tasks of mass monitoring of undergrowth over large areas, providing fast and accessible solutions. The Random Forest algorithm has demonstrated effectiveness in the work of Feduck *et al.* (2018) and Gan *et al.* (2023). The Random Forest algorithm appears most justified for processing two-dimensional images without point clouds or LiDAR. This approach has also proven more resistant to overfitting and requires only a limited amount of labeled data. The algorithm shows a smaller decline in model quality when working with similar data compared with neural networks.

This work tests and evaluates a methodology for monitoring individual undergrowth plants in the post-fire Amankaragay pine forest using UAV-based RGB channels as a more accessible alternative to multispectral image channels. To improve inventorying and monitoring of undergrowth recovery, this study compared the quality of manual validation with automated validation. This quality assessment enabled metric evaluation of each method's effectiveness.

This method is potentially limited in specific tasks compared with more complex architectures such as ResNet or SegFormer (Feduck *et al.*, 2018). Interseasonal validation and testing of this model were not carried out within the framework of this study. Results from the developed and tested model and its variations in other seasons may be distorted and require further work for clarification and validation.

Model classification is available only by morphological characteristics, without physiological indices. Based on the results of the conducted studies, to improve the model, it is recommended to investigate an algorithm for secondary data validation based on multispectral images, which would make it possible to describe the physiological state of the undergrowth. The following tasks were set in the course of the study:

1. Development and testing of an automated method for assessing forest cover recovery, in particular birch undergrowth, using the Amankaragay pine forest as an example, based on a UAV-mounted hybrid multispectral camera with RGB/G/R/RE/NIR channels and machine learning algorithms.
2. Obtaining data on undergrowth density in selected areas using the developed method.
3. Validation of manual and automated assessment.
4. Determination of the limitations and advantages of using this method, and development of recommendations for improving the accuracy class of the method for assessing undergrowth and vegetation mass objects.

MATERIALS AND METHODS

Study subjects

The subject of the present study is the Amankaragay pine forest, the largest isolated forest massif in the North Kazakhstan Region of the Republic of Kazakhstan (Wikipedia, the free encyclopedia., 2025). The forest lies in the southern part of the Kostanay, or North Turgay, Plain and occupies a considerable area along the steppe-forest boundary. The coordinates of the central part of the study area are 52°25′14.70″ N, 64°10′11.59″ E **(Figure 1)**.



Figure 1. Satellite image of the pine forest area

The formation of the landscape in this territory is determined by the alternation of alluvial and aeolian processes, resulting in the predominance of sandy ridges, sandy loams, and loams. The dominant soil-forming materials are white sands, sod-pine soils, and brown forest soils. The relief is characterized by gentle hills and shallow depressions that are temporarily moistened in spring (Baysholanov & S, 2017).

The main forest-forming species is Scots pine (*Pinus sylvestris*); however, after the fires of 2022, silver birch (*Betula pendula*) undergrowth, characterized by rapid vegetation growth during the first years of recovery, has been actively developing in burned areas. Aspen, shrubs, and mosaic patches of herbaceous vegetation are also present.

The area has a sharply continental climate, with hot, dry summers and long, cold winters. Average annual precipitation is approximately 300–350 mm, which contributes to the high fire hazard of forest lands, especially under drought conditions. From 2001 to 2019, 88 forest fires were recorded in the Amankaragay pine forest, covering more than 5,000 ha. The last major fire, in September 2022, was the largest in the region in the past 30 years (Wikipedia, the free encyclopedia., n.d.; Parliament of the Republic of Kazakhstan., 2003).

Ecological conditions after fire impact are characterized by severe degradation of ground cover, loss of the humus layer, reduced soil water-retention capacity, and accumulation of heavy metals in surface horizons. This creates prerequisites for changes in successional processes and transformation of phytocenoses. In this regard, the study area is a suitable example of forest territories exposed to acute technogenic and natural pressures. It serves as an appropriate model site for testing methods to monitor undergrowth recovery using UAVs and machine learning algorithms.

Within this study, tasks were set to survey seven forested and cleared sites, for each of which high-resolution orthophotomosaics were to be constructed. The table below presents the geographical location, spatial resolution, area, and coverage coordinates for each site (Ozgeldinova *et al.*, 2025).

Table 1. Spatial parameters of experimental sites for UAV monitoring, including pixel size, area, and coordinate coverage

No.	Object	X	Y	Pixel size X	Pixel size Y	Area (ha)	Coverage (coordinates)
1.1	Baganaly Forest 1	38459	15555	1.20487e-07	7.36897e-08	3.25	63.65997, 52.40575: 63.66460, 52.40689
1.2	Baganaly Forest 1.2	45074	12632	1.14611e-07	7.00928e-08	3.62	63.65983, 52.40508: 63.66499, 52.40596
1.3	Baganaly Forest 1.3	59097	8336	1.14603e-07	7.00970e-08	3.95	63.65975, 52.40474: 63.66652, 52.40532
2	Baganaly Clear-Cut 2	64424	33848	1.20527e-07	7.36862e-08	5.72	63.65463, 52.41790: 63.66240, 52.42039
3	Kalininskaya Clear-Cut 1	29554	27761	8.52777e-08	5.21207e-08	1.39	64.16615, 52.43305: 64.16867, 52.43450
4	Kalininskaya Clear-Cut 2	44005	55587	4.85182e-08	2.96551e-08	0.72	64.16897, 52.43155: 64.17111, 52.43320
5	Kalininskoye General Site	18451	14220	5.19005e-07	3.17222e-07	4.31	64.16419, 52.43110: 64.17377, 52.43561
6	Novonezhenka 1	35267	38930	1.69305e-07	1.03345e-07	2.31	64.07245, 52.49106: 64.07842, 52.49509
7	Novonezhenka 2	9999	13348	1.60476e-07	9.79513e-08	2.10	64.07641, 52.49246: 64.07801, 52.49377

DJI Mavic 3 Multispectral unmanned aerial vehicle

The DJI Mavic 3 Multispectral unmanned aerial vehicle **(Figure 2)**, equipped with a hybrid multispectral camera and multispectral sensors (RGB/G/R/RE/NIR), served as the main aerial survey tool for collecting primary spatial data.



Figure 2. DJI Mavic 3 Multispectral unmanned aerial vehicle in flight



Figure 3. Orthophotoplan of a burned forest area of the Amankaragay pine forest created using DJI Terra software

The team carried out mission setup and launch through the standard control interface, taking into account site parameters and the expected density of objects on the ground. The flight parameters were set as follows:

1. Flight altitude — 31 m, which provided a safe clearance above tree crowns and the required coverage area.
2. Spatial resolution, or ground sampling distance (GSD), — 1.45 cm/pixel, allowing individual trees and other vegetation objects to be detected and distinguished.

Image overlap: In areas with sparse vegetation, including cleared forest sites, we used standard settings: 80% frontal overlap and 70% side overlap. Under conditions of high woody-debris density and pronounced vertical structure, namely sites affected by fire, we applied increased overlap values of 90% in both directions. This ensured reliable image stitching during the construction of orthophotoplans and minimized potential data loss due to insufficient coverage of the survey area. After completing the fieldwork, all collected aerial photographic material was post-processed and structured for subsequent analysis.

Processing of orthophotoplan images (Orthophotomosaics)

Image processing was carried out using DJI Terra (DJI, n.d.), software designed to generate high-quality orthophotoplans, or orthophotomosaics, and reconstruct digital terrain models. For each test site, we created a separate project in the software, with the reconstruction mode set to "Visible Light." This mode reproduces the visual characteristics of vegetation objects as accurately as possible, which is critical when working with mosaics of forest structures and recognizing woody forms.

The projects were processed using standard reconstruction settings, including automatic exposure correction and overlap optimization. All images within one test site were automatically aligned and stitched into a single orthophotomosaic georeferenced to the WGS 84 coordinate system (EPSG.io., n.d.). The resulting orthophotoplans can be exported in GeoTIFF format while preserving high spatial resolution and ensuring a high level of unreferenced orthophotomosaic indicators. This minimizes spatial distortions in subsequent stages.

Figure 3 shows an orthophotoplan of a burned area of the Amankaragay pine forest (2.1 hectares), created using DJI Terra software.

To create the training sample in this study, we manually annotated orthophotos as polygons in QGIS (version 3.40.4). This approach ensured high-quality delineation of objects of interest, including seedlings, undergrowth, and other categories. Despite the advantage of this method compared with traditional image division into regular patches, several studies note the possibility of incomplete accounting of the full crown area due to the morphological characteristics of the objects (Buades *et al.*, 2005).

The term "patch" is widely used in machine learning to refer to local image fragments. These fragments are used in local classification and segmentation, or to form the feature space (Buades *et al.*, 2005).

To improve the model's generalization and increase the training sample size, we implemented a data augmentation procedure. Data augmentation includes applying geometric and photometric transformations to the original images. These include mirror reflections, rotations by fixed angles of 90°, 180°, and 270°, brightness and contrast adjustment, and adding noise, specifically Gaussian noise (Krizhevsky *et al.*, 2012; Shorten & Khoshgoftaar, 2019).

In this study, the augmentation procedure was implemented using the Rasterio library. Rasterio provides tools for working with georeferenced raster images. It enables reading, writing, spatial transformation, and metadata handling (Gillies, 2013).

This approach increases the diversity and robustness of the training sample. In addition, it speeds up data preparation for automated orthophoto analysis. Before augmentation, all images were manually categorized by class. This made it possible to create relevant synthetic examples for each object category. Thus, augmentation became an effective tool for improving model training and validation, especially with limited initial data.

Course of the study. data processing

Fieldwork with the study objects

For model training and independent validation, three study sites were selected: two homogeneous sites and one heterogeneous site. This approach ensures statistical independence of the test data and allows assessment of the models' transferability to sites with different vegetation structures.

Machine learning of the random forest model for creating tree-based decisions

The Random Forest algorithm, an ensemble machine learning method, was used to train the classification models. Ensemble methods involve simultaneously constructing and combining several base models, such as decision trees, to improve the accuracy, stability, and generalization of the final solution compared with a single model (Opitz & Maclin, 1999; Dietterich, 2000). In Random Forest, multiple decision trees are trained independently on different random subsamples of data and features, and the final class is determined by majority voting across all trees. This approach reduces the risk of overfitting and is particularly effective for high-dimensional, complex data. Breiman (2001) first proposed the Random Forest algorithm, and it is widely used in spatial data analysis, ecology, and remote sensing.

In addition, we tuned the key Random Forest hyperparameters during the study, particularly the number of trees in the ensemble. The optimal value of this parameter was selected based on the minimum error on the validation sample, which ensures a balance between model stability and computational efficiency.

To realize the advantages of this algorithm, the quality of the initial training sample is crucial. In this study, a vector mask was manually annotated for each seedling or undergrowth plant, covering only the inner and most clearly visible part of the crown, without including background and shadow pixels **(Figure 4)**. This approach ensures high purity of the training sample, although it may lead to slight underestimation of the full crown area (Gan *et al.*, 2023; Xi *et al.*, 2024). It provides higher object-delineation accuracy compared with dividing images into regular patches.

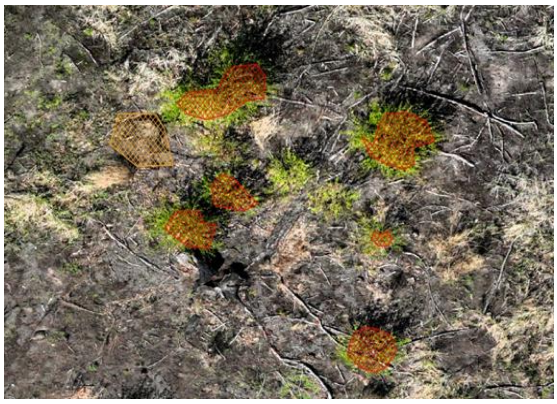


Figure 4. Example of polygonal annotation. UAV flight altitude: 31 m

To train the model, manual polygonal annotation of the orthophotoplan was carried out in QGIS version 3.40.4. Six object classes were identified within the study area of 2.5 hectares. Various objects were annotated polygonally:

1. 200 tree units based on the inner crown, excluding soil;
2. 200 polygons of green grass of different areas, each not exceeding 1 m^2;
3. 200 polygons of yellow grass of different areas, each not exceeding 1 m^2;
4. 200 polygons of moss of different areas, each not exceeding 0.5 m^2;
5. 200 polygons of tree stumps;
6. 200 land plots of different areas, each not exceeding 1 m^2.

Tree annotation was carried out along the inner crown, while soil was excluded to minimize the influence of background and shadow pixels. For other classes, polygons with areas close to the typical size of the corresponding vegetation type or element were used. The number 200 was selected as the maximum possible number for homogeneous and clearly distinguishable objects on this orthophotoplan, or orthophotomosaic, which ensures the statistical representativeness of the sample under spatial and morphological constraints. This uniform approach minimizes the initial class imbalance. Imbalance occurs when certain categories are represented by substantially more examples, which may reduce the identification accuracy of less represented classes (Buda *et al.*, 2018).

The patch size corresponded to the morphological characteristics of the selected objects and the spatial resolution of the images. This allowed full coverage of the target object and avoided including irrelevant background (Buades *et al.*, 2005). In this study, a patch is understood as a local image fragment corresponding to the annotated object or its immediate surroundings.

To improve recognition accuracy for the priority class, namely birch undergrowth, targeted data augmentation was applied. The number of patches for this class was increased using photometric transformations, including random brightness changes in the range from 0.8 to 1.2 and variation in the intensity of the green channel from 0.9 to 1.1. In addition, random noise, specifically Gaussian noise of 0.005–0.01, was added, which simulated the diversity of imaging conditions. This strategy aims to increase recall and recognition robustness for complex classes and aligns with the principles of cost-sensitive learning (He & Garcia, 2009). Despite the artificial imbalance in favor of the key class, this approach improves the overall efficiency and transferability of the models (Shorten & Khoshgoftaar, 2019).

Before augmentation, the original annotation and all patch variants were distributed in advance into training, validation, and test samples. Each patch and its modified versions were included in only one of these sets, preventing data leakage between the training and evaluation stages (Kaufman *et al.*, 2012). This control makes it possible to objectively assess the generalization ability of the models.

Moving on to the analysis of texture features, the following should be noted. All models were trained on a single image database, using the augmentation procedures described above. In particular, the same photometric transformations, including noise transformations, were applied to birch undergrowth, despite the potential reduction in the discriminative ability of texture features.

In this study, Haralick features were calculated based on the gray-level co-occurrence matrix (GLCM). Two key indicators were used: contrast and correlation (Haralick *et al.*, 1973). These features reflect the image's spatial heterogeneity and the statistical relationships between pixels. Haralick features are widely used in texture analysis in computer vision and remote sensing tasks (Clausi & Jernigan, 2000).

For model training, validation, and testing, the augmented patches were divided in a 0.7/0.15/0.15 ratio. This distribution is widely used in machine learning tasks because it provides

enough examples for training and allows objective assessment of model performance on independent samples (Kuhn & Johnson, 2013). It is especially important to maintain a fixed split before the augmentation stage to prevent identical patches from overlapping between training and test samples and to avoid data leakage.

Figure 5 shows the percentage ratio of the areas occupied by the objects.

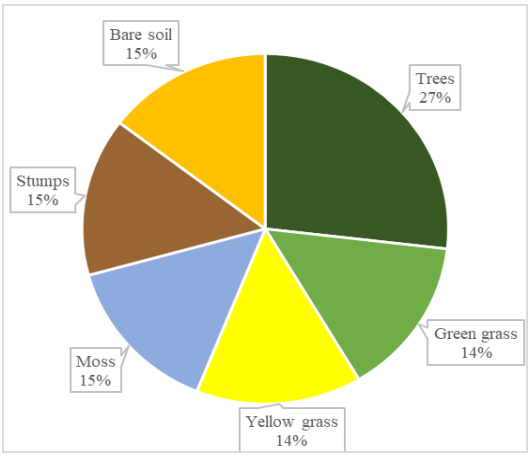


Figure 5. Percentage ratio of the areas occupied by the objects

Selection of model hyperconfiguration

Base model

The Random Forest algorithm, first proposed by Breiman (2001), was used to construct the base model. To ensure the reproducibility of the experiments, the random seed parameter was fixed at 42, which corresponds to accepted practice in machine learning and is recommended for correct model evaluation and comparison (Pedregosa *et al.*, 2011; Bouthillier *et al.*, 2021).

In the present study, the term "Base Model" refers to the standard implementation of Random Forest, in which only two hyperparameters were varied: target class weight and the number of decision trees (n_estimators). All other parameters remained at their default values. To construct the feature space in the Base Model, averaged values of the red, green, and blue channels (RGB) were extracted from each image, together with simple spectral indices traditionally used for vegetation analysis in digital images.

Excess Green (ExG) was calculated using the following formula:

$$E \times G = 2 \times G - R - B \quad (1)$$

Where R, G, and B are the values of the red, green, and blue channels, respectively.

This index emphasizes the intensity of green tones, which is especially characteristic of vegetation (Pedregosa *et al.*, 2011).

Excess Red (ExR) is defined by Formula (2) and identifies areas with a predominance of red color (Woebbecke *et al.*, 1995).

$$E \times R = 1.4 \times R - G \quad (2)$$

$E \times G - E \times R$ is the difference between ExG and ExR, allowing a clearer separation of areas with different predominance of green or red tones, which is important for identifying different types of vegetation cover. This set of features was selected due to its high informativeness in the classification of vegetation and background objects under RGB orthophotography conditions, as confirmed by its wide application in monitoring and remote sensing tasks (Meyer & Neto, 2008).

The optimal number of decision trees (n_estimators) was selected empirically. For each value of this parameter, the model was retrained, and its quality was evaluated on the validation sample using precision, recall, and F1-score metrics (Sokolova & Lapalme, 2009).

Out-of-bag error (OOB error) is a method for internally estimating the error of a Random Forest model without using a separate validation sample. It shows how well the model generalizes to data that were not used to build individual trees. Each tree is trained on its own subsample, and for some objects, called "out-of-bag" objects, the tree does not see them during training. **Figure 6** shows that the out-of-bag error decreases rapidly as the number of trees increases to 50–100, after which it plateaus. Reaching the OOB plateau means that the model, or its variation, has reached the minimum possible error.

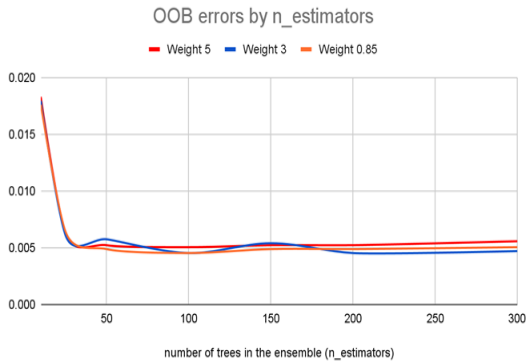


Figure 6. Effect of the number of trees in the ensemble on error depending on the weights of model variations

For the model variation with a target class weight of 5, the minimum error was achieved with a smaller number of trees than for the model variation with a target class weight of 3. This confirms the stability of ensemble methods when a sufficient number of base models is used (Dietterich, 2000; Sokolova & Lapalme, 2009). In the experiment, particular attention was paid to class balance: an increased weight was assigned to the priority class, "birch," in order to increase sensitivity to the target class under conditions of imbalance. This approach is widely used for imbalanced data (He & Garcia, 2009). For the model variation with a target class weight of 5, increasing the number of trees above 50 had almost no effect on the quality metrics, as shown in **Figure 6**.

For the model variation with a target class weight of 3, a similar quality "ceiling" was achieved at 100 trees. For the model variation with a target class weight of 0.85, a similar quality "ceiling" was also achieved at 100 trees. This is consistent with the known effects of ensemble methods: increasing the number of base models beyond a certain threshold does not substantially increase accuracy, while excessive complexity increases computational costs without a noticeable

improvement in results (Opitz & Maclin, 1999; Dietterich, 2000).

For the independent quality assessment of the base Random Forest model, or "Base Model," an orthophotomosaic of the homogeneous Kalininskaya 2 site, shown in **Figure 7**, was used. This site was not included in the training or validation samples. A manual count of the number of seedlings had been carried out in advance for this site, which made it possible to objectively compare the results of automatic and manual assessment.

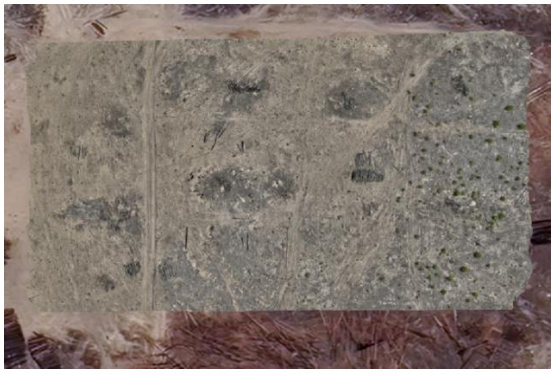


Figure 7. Homogeneous Kalininskaya 2 site for independent assessment

The graph in **Figure 8** presents the results of the Base Model at different target class weight values ("Weight"): the "Model Detection" columns show the number of seedlings identified by the model, while "Real Detection" shows the results of manual validation. These metrics were calculated using a heat map, which is described in the following sections.

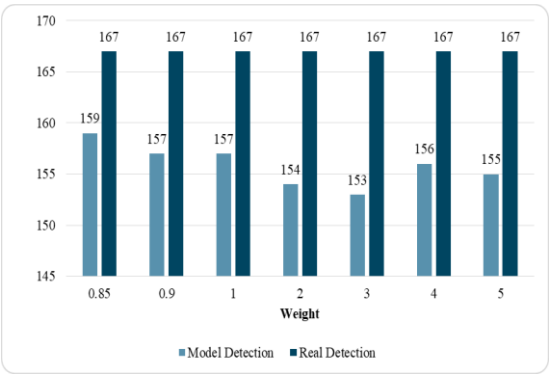


Figure 8. Comparison of automatic and manual seedling counts at different training weights of the target class

A comparative analysis of different model variants showed that the model variant with a target class weight of 0.85 was optimal. In this case, the deviation from the manual assessment results, in absolute terms, amounted to twelve objects, four of which were false positives (FP). A false positive is defined as a case in which the model incorrectly assigns an object to the target class. The model variation with a weight of 3 demonstrated a similar FP level; however, the best correspondence with the reference results was observed specifically for the model variation with a weight of 0.85. When the weight was increased to 5, FP increased to 5, along with greater discrepancies from the real data, indicating the onset of overfitting and reduced generalization.

To convert probabilistic predictions into binary labels, the optimal probability threshold BEST_THRESH = 0.563 was used, the same for all Base Model variations. This threshold was determined automatically on the validation sample to maximize the F1-score, which improves the balance between sensitivity, or recall, and specificity, or precision, under conditions of class imbalance. The use of an optimal threshold is more justified than the standard value of 0.5, especially for imbalanced data, as it provides a more objective assessment of classification effectiveness.

It should be noted that the obtained conclusions apply to the homogeneous site and the considered model configuration. The assessment of generalization and transferability of the results to heterogeneous sites is presented further in next section of this publication.

Modified model

As an alternative model variation, a "Modified Model" based on the Random Forest algorithm was implemented. Unlike the Base Model, which used standard spectral and morphological features as well as spectral indices, the Modified Model used two approaches to describe texture in images.

The first approach involves calculating statistical features from the gray-level co-occurrence matrix (GLCM), which estimates how often pairs of pixels with certain intensity values occur at a fixed distance and in a specified direction. Based on this matrix, texture characteristics such as contrast, energy, entropy, and homogeneity are extracted, making it possible to quantitatively describe spatial patterns of brightness distribution characteristic, for example, of different vegetation types, tree bark, or soil.

The second approach involves the recognition of local binary patterns (LBP), which transform the texture around each pixel into simple numerical codes reflecting sharp transitions between light and dark areas. This method effectively highlights details such as leaf edges or soil roughness. The combined use of these features allows object and structure types in orthophotos to be distinguished more accurately, provided that their appearance is complex and variable (Haralick *et al.*, 1973; Ojala *et al.*, 2002).

As in the Base Model, the random seed parameter was fixed at 42 to ensure the reproducibility of the experiments. The target class weight was set at 0.85, which had previously been identified as the optimal value. The optimal number of decision trees (*n_estimators*) was selected empirically, with a stepwise assessment of out-of-bag error (OOB error) on the validation sample.

Analysis of the results **(Figure 9)** showed that, for the Modified Model, increasing the number of trees to 300 provides a substantial reduction in OOB error and stabilization of model quality. This distinguishes it from the base configuration, where the error plateau was reached with a smaller number of trees.

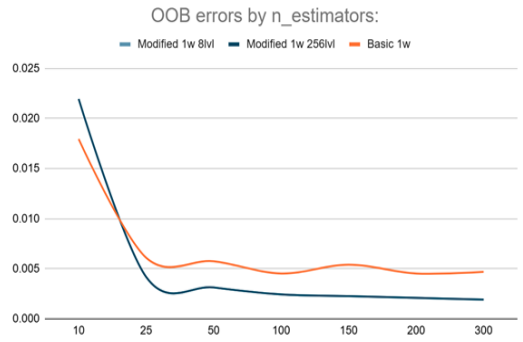


Figure 9. Effect of the number of trees in the ensemble on error depending on the weights and quantization levels of model variations

The increased complexity of the feature space associated with the expanded set of texture features requires a larger number of base models to achieve stable and accurate classification. This is consistent with conclusions on ensemble methods reported in the literature (Opitz & Maclin, 1999; Dietterich, 2000).

Figure 10 shows a comparison of the results of automatic and manual seedling detection at different quantization levels of RGB patches. The light-blue columns represent the number of objects identified by the Random Forest model. The dark-blue columns show the actual number of seedlings according to manual validation, namely 167 objects in all variants.

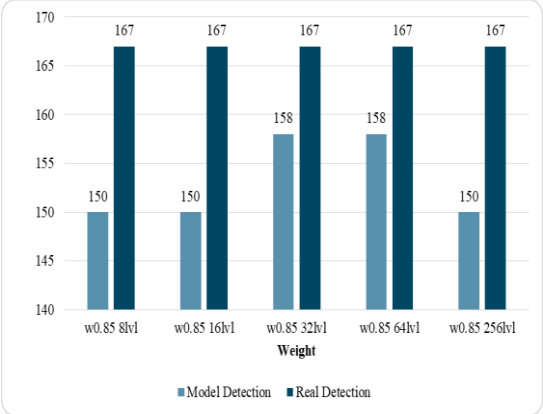


Figure 10. Comparison of automatic and manual counts of undergrowth plants, or seedlings, at different quantization levels (class weight = 0.85)

The same classification probability threshold, BEST_THRESH = 0.537, and target class weight of 0.85 were used in all experiments. Five quantization levels were analyzed: 8, 16, 32, 64, and 256.

At 8 and 16 quantization levels, the model identified 150 seedlings, which is 17 fewer than the reference value. This indicates a loss of important information under strong compression of color data.

At 32 and 64 levels, the number of detections increased to 158, which is 9 fewer than the reference value. This result demonstrates an optimal balance between detail and robustness to noise. At the maximum level of 256, the model again identified only 150 objects, which may indicate the influence of excessive detail on classification stability.

Thus, moderate quantization, at 32–64 levels, produced the smallest discrepancy with manual validation in the present study. This confirms that tuning the quantization parameter is critically important for reliable model performance under conditions of imbalanced classes. It also indicates low noise levels, which did not have a real effect on the training sample.

Binary heat map and density determination

In this study, a four-neighborhood connected-component clustering algorithm, or 4-neighborhood connectivity, was used to merge adjacent patches. This method combines neighboring patches that touch horizontally or vertically into one connected component, which is then interpreted as a separate object, in this case as one birch undergrowth plant. This approach avoids double or triple counting of overlapping patches and provides a more accurate quantitative assessment of objects. It also makes it possible to approximately convert the number of patches into the number of undergrowth plants.

To calculate the number of undergrowth plants, a heat map built from the results of the classification model was used, with a discrete patch size of 64 × 64 pixels. This size was selected in accordance with the previous stages of analysis and is optimal for the spatial resolution of the original orthophotos. In the present study, a heat map refers to the visual distribution of classes based on the initial data.

Figure 11 shows the original site before applying the heat map, while **Figure 12** shows the final heat map with marked clusters, clearly illustrating the process of identifying and counting undergrowth plants.



Figure 11. Image of the site without the heat map overlay



Figure 12. Image of the site with the heat map overlay

RESULTS AND DISCUSSION

The best individual variants of the base model and modified model have the metric characteristics presented in **Tables 1 and 2**.

Table 2. Metric characteristics of individual variants of the Base Model and Modified Model

Basic Model					Basic Model				
Object	**Precision**	**Recall**	**F-score**	**Support**	**Object**	**Precision**	**Recall**	**F-score**	**Support**
Birch	0.932	1	0.965	330	Birch	0.967	0.97	0.968	330
Green grass	0.663	0.6	0.63	180	Green grass	0.881	0.906	0.893	180
Yellow grass	0.757	0.9	0.822	180	Yellow grass	0.956	0.967	0.961	180
Moss	0.605	0.561	0.582	180	Moss	0.879	0.85	0.864	180
Stumps	0.766	0.872	0.816	180	Stumps	1	0.989	0.994	180
Soil	0.819	0.578	0.678	180	Soil	1	1	1	180
accuracy		0.782		1230	accuracy		0.95		accuracy
macro avg	0.757		0.752	0.749 1230	macro avg		0.947		1230
weighted avg	0.778		0.782	0.775 1230	weighted avg		0.95		1230
Best threshold	0.982	0.997	0.989	Value = 0.543	Best threshold	0.982	0.997	0.989	Value = 0.507

An interpretation of the tabular data is provided below. To evaluate the accuracy of the models and their variations, metrics were used based on the following logical outputs of the models:
True positive (TP): Seedlings that were marked and matched the annotation during model evaluation, measured in units;
False positive (FP): Objects that the model classified as seedlings but that were marked as other objects, measured in units;
False negative (FN): Objects that were marked as seedlings but that the model classified as another object, measured in units.
These logical outputs of the models made it possible to construct accuracy metrics for the models and their variations. The accuracy metrics and their definitions used in the present article are listed below.
Precision is a metric that reflects the proportion of tree detections without false positives, indicating the model's tendency toward false-positive results. The higher the value, the fewer over-selection errors occur. Excessively high values may be caused by a small amount of total data or by overfitting to a specific test site, according to previous sections of this publication.

$$Recall = \frac{TP}{TP + FN} \quad (3)$$

Recall is a metric that reflects the proportion of actually existing trees detected by the models. The higher the Recall value, the fewer original values are missed. Low Recall values may be due to insufficient annotation of objects of this class or overfitting to another class.

$$Precision = \frac{TP}{TP + FP} \quad (4)$$

F-Score is a metric that represents the average between the model's recall and precision, reflecting the model's balance between false positives and missed positive cases.

$$F - Score = 2 \times \frac{precision \times recall}{precision + recall} \quad (5)$$

Accuracy is a metric that reflects the proportion of correctly classified objects among the total number of observations.
Macro average (macro avg) is a metric that reflects the average value of logical metrics across all classes, regardless of their size.
Support is a metric that reflects the number of objects of each class used in metric calculation.
Best threshold is the value that indicates the probability threshold at which the maximum F1-score is achieved on the validation sample. This threshold is selected individually for each model and provides the optimal balance between sensitivity and specificity when working with imbalanced classes.
The combined use of the above metrics makes it possible to comprehensively evaluate classifier performance and correctly compare different model configurations.
Comparison of the base model and the modified model on the test sample (n = 1230) demonstrates a substantial advantage of the modified configuration across all key quality metrics. Both model variants were trained on the same data; however, the base model operates with simple spectral and morphological features, while the modified model includes an extended texture description based on GLCM and LBP.
The base model achieved an overall accuracy of 0.785, whereas the modified model achieved 0.947, corresponding to an absolute quality increase of 16.2 percentage points.
The improvement is noticeable across all polygonal objects, or classes, but is especially pronounced for "moss," where the F-score increased from 0.591 to 0.854; "green grass," from 0.649 to 0.896; and "soil," from 0.675 to 1.0. This indicates improved separability of difficult-to-distinguish classes, which is also confirmed by the increase in the macro average F-score from 0.753 to 0.945.
The macro average F1-score for the Base Model is 0.753, while for the Modified Model it is 0.945.
The weighted average F1-score changed from 0.778 to 0.947, reflecting improvement even under class imbalance.
For both models, an individual optimal probability threshold, or "Best threshold," was selected by maximizing the F1-score on the validation sample: 0.593 for the Base Model and 0.537 for

the Modified Model. This allows the best balance between sensitivity and specificity to be achieved.

The increase in the number of features and in model complexity was accompanied by an increase in processing time from 2 to 3 minutes; however, high computational efficiency was maintained for the full analysis of 1230 objects.

Within the framework of this study, two model architectures were implemented and tested: the Base Model and the Modified Model. The effectiveness of the models was evaluated on sites with different degrees of homogeneity and heterogeneity, selected as the Baganaly 2 and Kalininskaya 1 test sites **(Figures 13 and 14)**. This approach makes it possible to test the transferability and adaptability of the models across different landscape scenarios.

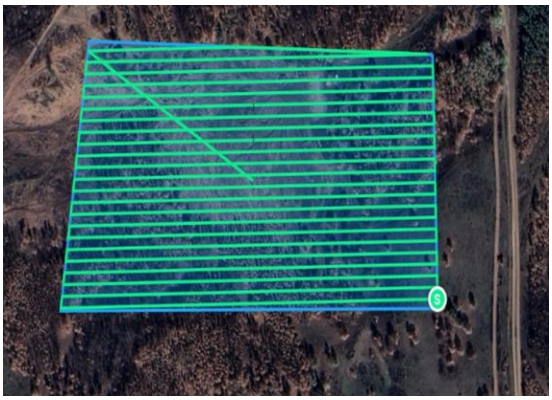


Figure 13. Flight trajectory and coverage scheme of the Baganaly-2 site during UAV-based aerial photography (GSD — 1.45 cm/pixel, area — 0.12 km^2)



Figure 14. Flight trajectory and coverage scheme of the Kalininskaya-1 site during UAV-based aerial photography (GSD — 1.45 cm/pixel, area — 15,596.3 m^2)

Analysis of the results presented in **Figure 15** demonstrates a substantial decrease in the number of false positives on heterogeneous sites when using the Modified Model compared with the Base Model. Thus, for heterogeneous data, the base models overestimate the number of target objects by more than 2–3 times relative to the actual value (492–575 versus 2). At the same time, the modified models, which use texture features and the optimal class weight, show a noticeable decrease in the number of erroneous detections (202–303). However, the absolute error remains high.

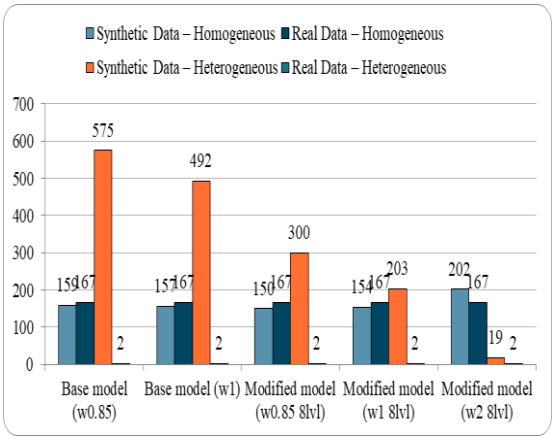


Figure 15. Comparison of variations of the two models

This difference in results between homogeneous and heterogeneous sites emphasizes the importance of accounting for the spatial structure and texture characteristics of images when solving problems of automatic classification of vegetation objects. The addition of texture features, such as GLCM and LBP, contributes to more accurate differentiation between target and background objects, especially under conditions of high landscape heterogeneity.

The obtained results indicate that even the most advanced variants of the Random Forest model remain sensitive to the characteristics of the sample. When the target class is extremely poorly represented on heterogeneous sites, the probability of overestimation remains. This indicates the need for further refinement of the approach, for example through the integration of additional contextual or multispectral features, the application of data-balancing methods, and the use of more complex ensemble and deep learning architectures. Recognition quality may also be improved by changing the dimensionality of heat-map sections. The conducted study demonstrates the potential of using complex feature spaces to improve the accuracy of automated undergrowth detection in orthophotos. It highlights the limitations of existing approaches as well as directions for further research. The full code for reproducibility is available at: https://github.com/Vel5id/qgis-forest-ml/ (GitHub, Inc. 2025).

CONCLUSION

The present study aimed to assess forest undergrowth using ultra-high-resolution orthophotos obtained from an unmanned aerial vehicle (UAV). To achieve this aim, an approach based on the Random Forest algorithm was developed in combination with expansion of the training sample through various data augmentation options and the use of a set of spectral and texture features, including GLCM and LBP metrics. The proposed methodology successfully addressed the stated task, making it possible to effectively identify undergrowth in aerial photographs. Particular attention was paid to the problem of class imbalance in order to improve the model's recognition of the target class, "birch." During training, this imbalance was compensated by adjusting class weight coefficients. These measures substantially increased the recall and precision of target-class detection, which is consistent with known evidence

that strong sample imbalance can significantly reduce the classification effectiveness of poorly represented classes while improving classification effectiveness for the target class.

The developed Random Forest classifier demonstrated high-quality recognition of undergrowth on test data. On homogeneous sites, the model achieved especially high accuracy in detecting the presence of undergrowth; on more complex heterogeneous sites, the quality decreased noticeably. All obtained cartographic results were verified by expert assessment through manual validation, which confirmed their reliability. The calculated quality metrics — accuracy, precision, recall, and F1-score — indicate reliable model performance. In particular, the high F1-score for the "undergrowth" class indicates that the classifier provides both high completeness of undergrowth detection and a low level of false positives, reflecting a balance between Precision and Recall.

Thus, the conducted study clearly demonstrated the possibility of effectively using UAV data to assess and map forest undergrowth. The obtained results are of important practical significance for forestry and vegetation monitoring: the proposed technology makes it possible to quickly and in detail identify the distribution of undergrowth over large areas without labor-intensive ground surveys. The use of combined spectral-texture features together with the Random Forest algorithm ensured high classification accuracy, thereby confirming the conclusions of other studies on the advantages of using texture features and expanding the remote sensing toolkit for forest ecosystem management tasks.

Nevertheless, the proposed approach has certain limitations. First, it was tested using data from only one region and under specific imaging conditions; further confirmation of its universality is needed for other types of forest ecosystems and different seasonal conditions. Second, drone-based orthophotos do not make it possible to "look" beneath a dense canopy; therefore, under a closed tree layer, the effectiveness of undergrowth detection may decrease. Third, during augmentation, the addition of noise in the range from 0.005 to 0.01 did not have a significant effect on model quality due to its low influence on 256-bit RGB channel values, which should be reconsidered in future work.

In the future, this study is planned to be expanded by including data from other sensors, such as multispectral imagery or LiDAR surveys, to account for the vertical structure of the forest, and by testing combinations of modern deep learning methods. This will improve the accuracy and robustness of undergrowth assessment and ensure the applicability of the method under a wider range of conditions.

ACKNOWLEDGMENTS: None

CONFLICT OF INTEREST: None

FINANCIAL SUPPORT: BR24992785 "Organization and implementation of comprehensive research to ensure sustainable development of the agro-industrial complex of the Kostanay region with the creation of a research and technology center".

ETHICS STATEMENT: None

REFERENCES

Akhmet, Zh. (2022). *Fire in Kostanay Region: Timeline of events*. Available from: https://otyrar.kz/2022/09/pozhar-v-kostanajskoj-oblasti-hronologiya-sobytij/

Banskota, A., Kayastha, N., Falkowski, M. J., Wulder, M. A., Froese, R. E., & White, J. C. (2014). Forest monitoring using Landsat time series data: A review. *Canadian Journal of Remote Sensing, 40*(5), 362-384. doi:10.1080/07038992.2014.987376

Baysholanov, S., & S (Eds.). (2017). *Agroclimatic resources of the Kostanay region: Scientific and applied reference book. Astana, 139 p*.

Bolbot, I. (2022). *Engulfed in flames: Kazakhstan struggles with the disaster and its aftermath.* Available from: https://vpoanalytics.com/2022/09/12/ohvachennye-ognem-v-kazahstane-boryutsya-s-bedstviem-i-ego-posledstviyami/

Bousquet, E., Mialon, A., Rodriguez-Fernandez, N., Mermoz, S., & Kerr, Y. (2022). Monitoring post-fire recovery of various vegetation biomes using multi-wavelength satellite remote sensing. *Biogeosciences, 19*(13), 3317-3336. doi:10.5194/bg-19-3317-2022

Bouthillier, X., Delaunay, P., Bronzi, M., Trofimov, A., Nichyporuk, B., Szeto, J., Sepahvand, N. M., Raff, E., Madan, K., Voleti, V., et al. (2021). Accounting for variance in machine learning benchmarks. *Proceedings of Machine Learning and Systems, 3*, 747-769. doi:10.48550/arXiv.2103.03098

Breiman, L. (2001). Random forests. *Machine Learning, 45*(1), 5-32. doi:10.1023/A:1010933404324

Buades, A., Coll, B., & Morel, J. M. (2005). A non-local algorithm for image denoising. In IEEE Computer Society Conference on Computer Vision and Pattern Recognition (CVPR'05) (Vol. 2, pp. 60-65). New York, NY: IEEE. doi:10.1109/CVPR.2005.38

Buda, M., Maki, A., & Mazurowski, M. A. (2018). A systematic study of the class imbalance problem in convolutional neural networks. *Neural Networks, 106*, 249-259. doi:10.1016/j.neunet.2018.07.011

Bugubaeva, A., Chashkov, V., Mamikhin, S., Kuprijanov, A., Kuanyshbaev, S., Nugmanov, A., Bulaev, A., Shcheglov, A., Manakhov, D. V., Zharlygasov, Zh., et al. (2023). Assessment of the state of vegetation cover of recultivated dumps of uranium deposits in Northern Kazakhstan. *Brazilian Journal of Biology, 83*(5), 1-17. doi:10.1590/1519-6984.279616

Chashkov, V. N., Kuanyshbayev, S. B., Bugubayeva, A. U., & Bashev, A. V. (2023). Main approaches to monitoring the effect of diffuse surface run off from agricultural fields on the water quality of the Karatomar Reservoir using Earth's remote sensing. *3i: intellect, idea, innovation – intellekt, ideya, innovatsiya, 3*, 108-118. doi:10.52269/22266070_2024_3_108

Chashkov, V., Bugubaeva, A., Kuprijanov, A., Bulaev, A., Mamikhin, S., Joldassov, A., Shcheglov, A., & Paramonova, T. (2024). Formation of vegetation cover and soil quality indicators at the mine sites of a gold-bearing deposit (the case of Kara-Agash, Kazakhstan). *OnLine Journal of Biological Sciences, 24*(4), 877-887. doi:10.3844/ojbsci.2024.877.887

Clausi, D. A., & Jernigan, M. E. (2000). Designing Gabor filters for optimal texture separability. *Pattern Recognition, 33*(11), 1835-1849. doi:10.1016/S0031-3203(99)00181-8

Dancheva, A. V., Zalesov, S. V., & Portyanko, A. V. (2015). Assessment of the successfullness of post-fire forest regeneration of pine forest in Northern Kazakhstan. *Aktual'nye problemy lesnogo kompleksa, 43*, 77-79.

Dietterich, T. G. (2000). Ensemble methods in machine learning. In Multiple classifier systems (pp. 1-15). Berlin, Heidelberg: Springer. doi:10.1007/3-540-45014-9_1

DJI. (n.d.). *DJI Terra*. Available from: https://enterprise.dji.com/dji-terra

Dosanova, A. (2022). *The UAE has allocated $1 million for forest restoration in the Kostanay region*. Available from: https://the-steppe.com/novosti/oae-vydelili-million-dollarov-na-vosstanovlenie-lesov-v-kostanayskoy-oblasti

EPSG.io. (n.d.). *EPSG:32641 – WGS 84 / UTM zone 41N*. Available from: https://epsg.io/32641

Feduck, C., McDermid, G. J., & Castilla, G. (2018). Detection of coniferous seedlings in UAV imagery. *Forests, 9*(7), 432. doi:10.3390/f9070432

Gan, Y., Wang, Q., & Iio, A. (2023). Tree crown detection and delineation in a temperate deciduous forest from UAV RGB imagery using deep learning approaches: Effects of spatial resolution and species characteristics. *Remote Sensing, 15*(3), 778. doi:10.3390/rs15030778

Gillies, S. (2013). *Rasterio: Geospatial raster I/O for Python programmers*. Available from: https://rasterio.readthedocs.io/en/latest/

Gribanov, L. N. (1960). *Steppe pine forests of the Altai region and Kazakhstan. Moscow-Leningrad: Goslesbumizdat, 156 p*.

Haralick, R. M., Shanmugam, K., & Dinstein, I. H. (1973). Textural features for image classification. *IEEE Transactions on Systems, Man, and Cybernetics, SMC-3*(6), 610-621. doi:10.1109/TSMC.1973.4309314

He, H., & Garcia, E. A. (2009). Learning from imbalanced data. *IEEE Transactions on Knowledge and Data Engineering, 21*(9), 1263-1284. doi:10.1109/TKDE.2008.239

Jolly, W., Cochrane, M., Freeborn, P., Holden, Z. A., Brown, T. J., Williamson, G. J., & Bowman, D. M. J. S. (2015). Climate-induced variations in global wildfire danger from 1979 to 2013. *Nature Communications, 6*, 7537. doi:10.1038/ncomms8537

Kaufman, S., Rosset, S., & Perlich, C. (2012). Leakage in data mining: Formulation, detection, and avoidance. In Proceedings of the 17th ACM SIGKDD International Conference on Knowledge Discovery and Data Mining (pp. 556-563). New York, NY: Association for Computing Machinery. doi:10.1145/2020408.2020496

Kleinsmann, J., Verbesselt, J., & Kooistra, L. (2023). Monitoring individual tree phenology in a multi-species forest using high resolution UAV images. *Remote Sensing, 15*(14), 3599. doi:10.3390/rs15143599

Krizhevsky, A., Sutskever, I., & Hinton, G. E. (2012). ImageNet classification with deep convolutional neural networks. In F. Pereira, C. J. C. Burges, L. Bottou, & K. Q. Weinberger (Eds.), Advances in neural information processing systems (Vol. 25, pp. 1097-1105). Red Hook, NY: Curran Associates, Inc.

Kuhn, M., & Johnson, K. (2013). *Applied predictive modeling*. New York, NY: Springer. doi:10.1007/978-1-4614-6849-3

Kupriyanov, A. N., Trofimov, I. T., Zablotskiy, V. I. (2003). *Restoration of forest ecosystems after fires*. KREOO Irbis.

Logachev, M. (2024). Functional requirements for an intelligent system for monitoring the impact of beaver activity on ecosystems. *BIO Web of Conferences, 130*, Article 08022. doi:10.1051/bioconf/202413008022

Makarov, A. (2022). *Fires in Kazakhstan's Kostanay region: A complete timeline*. Available from: https://bizmedia.kz/2022/09/05/pozhary-v-kostanajskoj-oblasti-hronologiya

Makhanova, N. B., Berdenov, Zh. G., Sansyzbayeva, A. B., & Sagynbayeva, A. B. (2022). Assessment of the structural dynamics of the Amankaragai pine forest using remote sensing data. *Journal of Geography and Environmental Management, 66*(3), 17-27. doi:10.26577/JGEM.2022.v66.i3.02

Meyer, G. E., & Neto, J. C. (2008). Verification of color vegetation indices for automated crop imaging applications. *Computers and Electronics in Agriculture, 63*(2), 282-293. doi:10.1016/j.compag.2008.03.009

Nasha Gazeta. (2022). *Burnt forests in the Kostanay region have begun to be restored*. Available from: https://www.ng.kz/modules/news/article.php?storyid=46940

Nugmanov, A. B., Mamikhin, S., Valiev, Kh. Kh., Bugubaeva, A. U., Tokusheva, A. S., Tulkubaeva, S. A., & Bulaev, A. (2022). Poly-species phytocenoses for ecosystem restoration of degraded soil covers. *OnLine Journal of Biological Sciences, 22*(3), 268-278. doi:10.3844/ojbsci.2022.268.278

Official website of the President of the Republic of Kazakhstan. (2022). *During a meeting of the operational headquarters for fire suppression in the Kostanay region, President of the Republic of Kazakhstan Kassym-Jomart Tokayev emphasized the need to develop and implement a set of measures to restore forest resources and ensure preventive work to prevent similar crises in the future*. Available from: http://president.kz/ru/prezident-provel-zasedanie-operativnogo-shtaba-po-likvidacii-pozharov-v-kostanayskoy-oblasti-58212

Ojala, T., Pietikäinen, M., & Mäenpää, T. (2002). Multiresolution gray-scale and rotation invariant texture classification with local binary patterns. *IEEE Transactions on Pattern Analysis and Machine Intelligence, 24*(7), 971-987. doi:10.1109/TPAMI.2002.1017623

Opitz, D., & Maclin, R. (1999). Popular ensemble methods: An empirical study. *Journal of Artificial Intelligence Research, 11*, 169-198. doi:10.1613/jair.614

Ozgeldinova, Z., Mukayev, Z., Zhanguzhina, A., Ulykpanova, M., & Aidarkhanova, G. (2025). Impact of forest fire on the heavy metal content in the soil cover of the Amankaragay pine forest, Kostanay Region. *Journal of Ecological Engineering, 26*(3), 350-364. doi:10.12911/22998993/199472

Parliament of the Republic of Kazakhstan. (2003). *Forest Code of the Republic of Kazakhstan of July 8, 2003, No. 477*. Available from: https://adilet.zan.kz/rus/docs/K030000477_

Pedregosa, F., Varoquaux, G., Gramfort, A., Michel, V., Thirion, B., Grisel, O., Blondel, M., Prettenhofer, P., Weiss, R., Dubourg, V., et al. (2011). Scikit-learn: Machine learning in Python. *Journal of Machine Learning Research, 12*, 2825-2830. doi:10.48550/arXiv.1201.0490

Pugachev, P. G. (1994). *Pine forests of the Turgay depression*. Kostanayskiy pechatnyy dvor.

Shorten, C., & Khoshgoftaar, T. M. (2019). A survey on image data augmentation for deep learning. *Journal of Big Data, 6*(1), 60. doi:10.1186/s40537-019-0197-0

Sokolova, M., & Lapalme, G. (2009). A systematic analysis of performance measures for classification tasks. *Information Processing & Management, 45*(4), 427-437. doi:10.1016/j.ipm.2009.03.002

Sputnik. (2022). *Forest restoration efforts are underway in Kostanay Oblast following a major fire, the mayor said*. Available from: https://ru.sputnik.kz/20221004/v-kostanayskoy-oblasti-nachinayut-vosstanavlivat-les-posle-krupnogo-pozhara---akim-28152373.html

Van der Werf, G. R., Randerson, J. T., Giglio, L., van Leeuwen, T. T., Chen, Y., Rogers, B. M., Mu, M., van Marle, M. J. E., Morton, D. C., Collatz, G. J., et al. (2017). Global fire emissions estimates during 1997–2016. *Earth System Science Data, 9*, 697-720. doi:10.5194/essd-9-697-2017

Wikipedia, the free encyclopedia. (2025). *Amankaragay forest*. Available from: https://ru.wikipedia.org/wiki/%D0%90%D0%BC%D0%B0%D0%BD%D0%BA%D0%B0%D1%80%D0%B0%D0%B3%D0%B0%D0%B9%D1%81%D0%BA%D0%B8%D0%B9_%D0%B1%D0%BE%D1%80

Wikipedia, the free encyclopedia. (n.d.). *2023 Kazakhstan wildfires*. Available from: https://en.wikipedia.org/wiki/2023_Kazakhstan_wildfires

Woebbecke, D. M., Meyer, G. E., Von Bargen, K., & Mortensen, D. A. (1995). Color indices for weed identification under various soil, residue, and lighting conditions. *Transactions of the ASAE, 38*(1), 259-269. doi:10.13031/2013.27838

Xi, Z., Hopkinson, C., & Chasmer, L. (2024). Supervised terrestrial to airborne laser scanner model calibration for 3D individual-tree attribute mapping using deep neural networks. *ISPRS Journal of Photogrammetry and Remote Sensing, 209*, 324-343. doi:10.1016/j.isprsjprs.2024.02.010

Zarubin, M., Kuanyshbayev, S., Chashkov, V., Yskak, A., Nugmanov, A., Salykova, J., Bashev, A., & Nurpeisov, A. (2025a). Assessing the accuracy of 3D modeling of hydrotechnical structures using bathymetric drones: A study of the Karatomara Reservoir. *Sustainability, 17*(11), 4858. doi:10.3390/su17114858

Zarubin, M., Kuanyshbayev, S., Chashkov, V., Yskak, A., Nugmanov, A., Salykova, O., Bashev, A., & Nurpeisov, A. (2025b). On the question of assessing the accuracy of 3D modeling of water reserves using the example of the Karatomar Reservoir. *Preprints, 2025040253*. doi:10.20944/preprints202504.0253.v1